JOURNAL OF SOLID STATE CHEMISTRY 22, 71–75 (1977)

Ferromagnetic Anti-PbFCl-Type ZnMnSb

V. JOHNSON AND W. JEITSCHKO*

Central Research and Development Department,† Experimental Station, E. I. du Pont de Nemours and Company, Wilmington, Delaware 19898

Received February 9, 1977

In the $Zn_xMn_{2-x}Sb$ system, the tetragonal, anti-PbFCl structure occurs between Mn_2Sb and ZnMnSb. The latter is essentially an ordered compound with Zn occupying the ninefold coordinated site (II), and Mn the tetrahedral layer positions (I). Magnetic measurements indicate ferromagnetic ordering of Mn as in isostructural AlMnGe, GaMnGe, and the Mn(I) substructure of ferrimagnetic Mn_2Sb. The observed moment of ZnMnSb and the $Zn_xMn_{2-x}Sb$ single-phase field are consistent with the unusual low spin d^6 configuration (+1 formal oxidation state) postulated for Mn(I) in Mn_2Sb, AlMnGe, and GaMnGe.

Introduction

In tetragonal Mn_2Sb (Cu_2Sb or anti-PbFCl structure), two different cation sites, I and II, are present. Since Sb is trivalent, one manganese cation (I) is monovalent, the other (II) divalent (*1*). This inference is supported by neutron diffraction measurements (*2*) which show magnetic moments of $2.13 \pm 0.20\ \mu_B$ for Mn(I) and $-3.87 \pm 0.40\ \mu_B$ for Mn(II). If this valence formulation is correct, divalent cations of similar size should substitute for Mn(II). One such is Zn^{2+} and we report here preparation, structure, and properties of $Zn_xMn_{2-x}Sb$ compositions as part of our effort to systematize formal valences and bonding in both PbFCl and anti-PbFCl-type compounds.

Experimental

Sample preparation. $Zn_xMn_{2-x}Sb$ compositions were prepared from the elements. Zn (pieces), Mn (pieces), and Sb (powder) (all >99% pure) were reacted in the desired stoichiometry in evacuated and sealed silica tubes at temperatures between 500 and 700°C. The silica tubes were lined with high purity alumina crucibles. Most samples were heated at 50°C/hr from 200 to 700°C, held at 700°C for 16 hr, cooled rapidly to 500°C, and held for 2½ days. Homogeneous, well-crystallized products resulted which contained well-developed crystal grains. In the case of ZnMnSb, these crystals were used for structural and electrical characterization.

Phase analysis. Powder X-ray diffraction techniques were used for phase identification and lattice constant measurements. Most samples were characterized by an automatic powder diffractometer with CuKα radiation and a graphite monochromator. A Guinier-Hägg camera, David–Mann film reader, and a least-squares computer program were used for precision lattice constant determination.

Magnetic and electrical measurements. Magnetic measurements were performed between 4.2 and 400°K with a PAR vibrating sample magnetometer. Electrical measurements were made over the same temperature range on a single crystal bar, 0.039 mm ×

* Present address: Institute for Inorganic and Analytical Chemistry, University of Giessen, D-63 Giessen, Federal Republic of Germany.

† Contribution No. 2445.

ISSN 0022–4596

0.013 mm × 0.005 mm, by a four-probe technique using soldered indium contacts.

Structure refinement. Single crystals of ZnMnSb were examined in a Buerger precession camera with MoKα radiation. They show 4/mmm diffraction symmetry and the space group extinctions ($hk0$ observed only when $h + k = 2n$) are characteristic for space group $P4/nmm$, the space group of the PbFCl-type structure. The crystal used for the structure refinement was taken from a sample with lattice constants $a = 4.1726$ (*2*), $c = 6.2332$ (*4*) Å (high-purity KCl standard: $a = 6.2931$ Å). It had irregular shape which, for the purpose of absorption correction, was approximated with a sphere of radius 0.025 mm. Intensity data were collected on an automated four-circle diffractometer with Zr-filtered Mo radiation. Scans were along 2 θ with a scan angle of 2° and a scan speed of 1.5° 2 θ/min. Background was counted for 20 sec at both sides of each scan. All reflections up to 70° 2 θ were measured and equivalent reflections were averaged to reduce absorption errors due to deviations from spherical crystal shape.

The structure was refined with a full-matrix least-squares program (*3*). Atomic scattering factors for neutral atoms (*4*) were used, corrected for anomalous dispersion (*5*). Weights were assigned according to counting statistics. For the initial least-squares cycles the atom distribution and positional parameters for AlMnGe (*6*) were used. In (anti-)PbFCl-type phases fractional occupancies for those sites which correspond to the Mn and the Zn positions in ZnMnSb are occasionally found. Therefore, occupational parameters for those positions were also varied, while the occupancy of the Sb position was held constant to fix the overall scale factor.

Results

Single-phase anti-PbFCl-type phases were observed between compositions Mn_2Sb and ZnMnSb on the basis of X-ray powder diffraction diagrams. Observed and calculated *d*-spacings for ZnMnSb are given in Table I.

TABLE I

OBSERVED AND CALCULATED *d*-SPACINGS FOR ZnMnSb, $a = 4.173$ Å, $c = 6.233$ Å, SPACE GROUP $P4/nmm$

hkl	d_{obs} (Å)	Q_{obs}[a]	Q_{calc}	I_{obs}
001	6.224	0.0258	0.0257	5
101	3.4665	0.0832	0.0837	70
002	3.1155	0.1030	0.1030	70
110	2.9508	0.1148	0.1149	80
111	2.6669	0.1406	0.1406	75
102	2.4962	0.1605	0.1604	10
112	2.1431	0.2177	0.2178	100
200	2.0868	0.2296	0.2297	90
003	2.0781	0.2316	0.2316	45
103	1.8596	0.2892	0.2891	10
211	1.7878	0.3129	0.3129	35
202	1.7338	0.3326	0.3327	60
113	1.6988	0.3465	0.3465	5
212	1.6073	0.3900	0.3901	2
004	1.5583	0.4118	0.4118	25
220	1.4752	0.4595	0.4595	65
203	1.4724	0.4613	0.4613	60
104	1.4602	0.4690	0.4692	2
213	1.3884	0.5188	0.5188	5
114	1.3777	0.5268	0.5267	5
301	1.3574	0.5427	0.5426	5
222	1.3334	0.5625	0.5624	25
310	1.3195	0.5744	0.5744	25
311	1.2908	0.6002	0.6000	15
204	1.2484	0.6416	0.6416	35

[a] $Q = 1/d^2$.

Compositions richer in Zn than ZnMnSb contained the anti-PbFCl-type phase in addition to other phases; furthermore, lattice constants of the anti-PbFCl phase in these Zn-rich compositions were close to those of

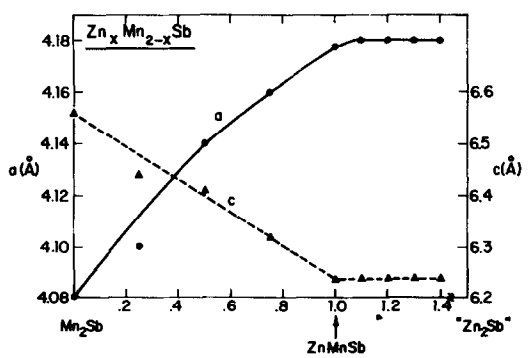

FIG. 1. Cell dimensions of $Zn_xMn_{2-x}Sb$ compositions.

TABLE II

STRUCTURAL PARAMETERS OF ZnMnSb[a]

P4/nmm	Occupancy	x	y	z	$b_{11} = b_{22}$	b_{33}	$B(A^2)$
Mn 2a	0.889 (14)	$\frac{1}{4}$	$\frac{3}{4}$	0	0.0118 (12)	0.0057 (8)	0.84
Zn 2c	0.942 (15)	$\frac{1}{4}$	$\frac{1}{4}$	0.2808 (5)	0.0159 (11)	0.0110 (8)	1.31
Sb 2c	1	$\frac{1}{4}$	$\frac{1}{4}$	0.7160 (3)	0.0101 (5)	0.0075 (3)	0.86

[a] Numbers in parentheses are estimated standard deviations in the least significant digits. Thermal parameters are of the form $T = \exp(-\Sigma\Sigma\, h_i h_j b_{ij})$. The last column contains equivalent B values.

ZnMnSb (Fig. 1). ZnMnSb is therefore a terminal composition suggesting ordering of Mn and Zn on the two crystallographic positions for the metal atoms.

This was essentially confirmed by the crystal structure refinement, the results of which are summarized in Table II. [The conventional R-value (for F-values) for this refinement is 0.050 for the total of 168 unique reflections and $R = 0.044$ for the 141 reflections with F values greater than three standard deviations. A list of observed and calculated structure amplitudes is available.[1]] Both the Mn and the Zn positions were found with less than full occupancy. This result can be interpreted in two ways with respect to the ordering of the Mn and Zn atoms on the two cation sites. Either the Mn and Zn atoms occupy only their respective sites, then both sites have slight deviations from full occupancy as shown in Table II. Or, if the Mn and Zn atoms have a strong tendency for disorder, the "Zn position" could contain as much as 35% Mn with the remaining 65% occupied by Zn. Assuming equal amounts of Zn and Mn in the compound, the "Mn position" would then contain 57% Mn, 27% Zn, and 16% of that site would remain unoccupied.

[1] "See NAPS Document No. 03027 for one page of supplementary material. Order form ASIS/NAPS c/o Microfiche Publications, P.O. Box 3513, Grand Central Station, New York, N.Y. 10017. Remit in advance for each NAPS accession number. Make checks payable to Microfiche Publications." Photocopies are $5.00. Microfiche are $3.00. Outside of the U.S. and Canada, postage is $3.00 for a photocopy or $1.00 for a fiche.

TABLE III

INTERATOMIC DISTANCES (Å) IN ZnMnSb[a]

Mn: 4Sb 2.736	Zn: 1Sb 2.712	Sb: 4Mn 2.736
4Zn 2.723	4Sb 2.951	1Zn 2.712
4Mn 2.950	4Mn 2.723	4Zn 2.951

[a] All distances shorter than 3.5 Å are given. Standard deviations are less than 0.001 Å.

Zn is in square pyramidal coordination with respect to the Sb atoms while the smaller Mn atom is approximately tetrahedrally coordinated by Sb (Table III). The PbFCl-type structure contains another tetrahedrally coordinated site which is occupied by Cu atoms in the filled PbFCl-type compound ZrCuSiAs (7). The possibility that Mn atoms occupy that site in ZnMnSb can be excluded: At least-squares refinement of the structure with Mn atoms on that site resulted in an occupancy parameter of -0.014 ± 0.012 for that position.

ZnMnSb is a ferromagnet with $T_c = 302°K$ (Fig. 2). The ferromagnetic moment measured

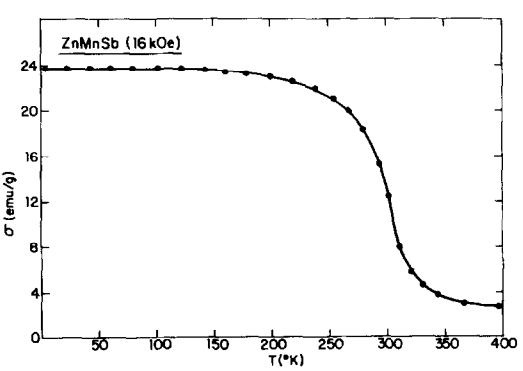

FIG. 2. Magnetization vs temperature for ZnMnSb.

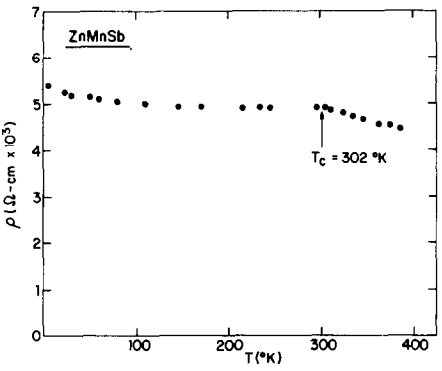

FIG. 3. Electrical resistivity of ZnMnSb.

at 4.2°K on powder samples is 1.2 μ_B/Mn for the nominal composition ZnMnSb or 1.32 μ_B/(Mn atom) assuming 0.9 (Mn atoms)/ formula unit, as suggested by the structure refinement. The highest field used in the measurement was 16 kOe, hence these values might be low. Magnetic properties for the other anti-PbFCl-type $Zn_xMn_{2-x}Sb$ compositions were not studied.

Electrical resistivity data (Fig. 3) show ρ decreasing slowly with T below T_c and a slightly more rapid decrease above. An activation energy of ~0.01 eV was calculated from the data above T_c. The Seeback coefficient α, measured at room temperature is low (−10 μV/°K), hence firm conclusions as to the conductivity type of ZnMnSb will have to await further study on purer and more defect-free samples.

Discussion

Among the binary antimonides of the transition metals, only Mn_2Sb and Cu_2Sb have the anti-PbFCl structure. The composition ZnMnSb may therefore be regarded as the terminal member of a pseudobinary field which lacks the end member "Zn_2Sb". On the other hand, since Mn and Zn are ordered on the I and II sites, respectively, ZnMnSb is a ternary compound, albeit exhibiting nonstoichiometry on the basis of occupancies observed in the structure determination. In the solid solution $Zn_xMn_{2-x}Sb$ between Mn_2Sb and ZnMnSb, we would expect Zn to substitute for Mn(II).

The results of the structure refinements of ZnMnSb indicate partial occupancies of the Mn and possibly also the Zn position. Partial occupancies for these sites are known for other PbFCl-type compounds (*8*). On the basis of interatomic distances alone, it is difficult to say which of the two sites should show a preference for the formation of vacancies. All atoms have high coordination and many relatively short Mn–Zn interactions indicate bonding characteristics of intermetallic compounds. Thus some disorder between Zn and Mn is likely to occur which will influence both the magnetic and electrical properties.

Between Mn_2Sb and ZnMnSb, the a axis increases and c decreases (Fig. 1). The cell volume changes very slightly, however, while c/a and the Mn(I)–Mn(I) distances change appreciably (Table IV). These increased Mn(I)–Mn(I) distances in ZnMnSb could lead to narrower d bands than in Mn_2Sb which will also change both conductivity and magnetic properties.

The strong preference of Mn for the tetrahedral layer position (I) is indicated by the

TABLE IV

TERNARY ANTI-PbFCl-TYPE COMPOUNDS

Compound	a (Å)	c (Å)	c/a	Mn–Mn (Å)	T_c (K)	Magnetic moment μ_B Mn (I)	Ref.
Mn_2Sb	4.08	6.56	1.61	2.88	550	2.13 ± 0.20 Mn I −3.87 ± 0.40 Mn II	*2*
ZnMnSb	4.17	6.23	1.49	2.96	302	1.2	This work
AlMnGe	3.92	5.95	1.52	2.77	518	1.52	*6*
GaMnGe	3.97	5.88	1.48	2.81	458	1.66	*9*

termination of the single-phase field at ZnMnSb. Zn apparently does not enter the I position since metal–metal bonding via *d*-electrons stabilizes these layers. Atoms in these layers are known to exhibit unusual valence states as a result of intralayer bonding, e.g., NbSiAs (*10*) and ZrSiS (*11*). The unusual formal oxidation state of +1 for Mn in ZnMnSb (and also AlMnGe and GaMnGe) can therefore be rationalized. For Mn^{1+} (d^6) in the covalent antimonides and germanides, we might expect a low-spin configuration with a maximum magnetic moment of 2 μ_B for tetrahedral coordination. The observed moments for ZnMnSb as well as AlMnGe and GaMnGe (Table IV) are less than this value probably due to some disorder between the I and II sites as well as delocalization of the *d*-states. The disorder in combination with nonstoichiometry might also explain the "extrinsic" appearing conductivity (Fig. 3) of ZnMnSb.

Acknowledgments

We are grateful to C. Poole for assistance in synthesis, J. Gillson for the electrical measurements, C. G. Frederick for the magnetic measurements, and D. M. Graham with the crystallographic work.

References

1. J. B. GOODENOUGH, "Magnetism and the Chemical Bond," p. 290, Interscience, New York (1963).
2. M. K. WILKINSON, N. S. GINRICH, AND C. G. SHULL, *J. Phys. Chem. Solids* **2**, 289 (1957).
3. L. W. FINGER, Computer program for the least-squares refinement of crystal structures, unpublished.
4. D. T. CROMER AND J. B. MANN, *Acta Cryst. A* **24**, 321 (1968).
5. D. T. CROMER AND D. LIBERMAN, *J. Chem. Phys.* **53**, 1891 (1970).
6. N. S. SATYA MURTHY, R. J. BEGUM, C. S. SOMANATHAN, AND M. R. L. N. MURTHY, *J. Appl. Phys.* **40**, 1870 (1969).
7. V. JOHNSON AND W. JEITSCHKO, *J. Solid State Chem.* **11**, 161 (1974).
8. W. JEITSCHKO, P. C. DONOHUE, AND V. JOHNSON, *Acta Cryst. B* **32**, 1499 (1976).
9. G. BRYAN STREET, *J. Solid State Chem.* 7(3), 316 (1973).
10. V. JOHNSON AND W. JEITSCHKO, *J. Solid State Chem.* **6**, 306 (1973).
11. A. J. KLEIN HANEVELD AND F. JELLINEK, *J. Less Common Metals* **18**, 123 (1969).